

BackEISNN: A Deep Spiking Neural Network with Adaptive Self-Feedback and Balanced Excitatory-Inhibitory Neurons

Dongcheng Zhao, Yi Zeng, and Yang Li

Abstract—Spiking neural networks (SNNs) transmit information through discrete spikes, which performs well in processing spatial-temporal information. Due to the non-differentiable characteristic, there still exist difficulties in designing well-performed SNNs. Recently, SNNs trained with backpropagation have shown superior performance due to the proposal of the gradient approximation. However, the performance on complex tasks is still far away from the deep neural networks. Taking inspiration from the autapse in the brain which connects the spiking neurons with a self-feedback connection, we apply an adaptive time-delayed self-feedback on the membrane potential to regulate the spike precisions. As well as, we apply the balanced excitatory and inhibitory neurons mechanism to control the spiking neurons' output dynamically. With the combination of the two mechanisms, we propose a deep spiking neural network with adaptive self-feedback and balanced excitatory and inhibitory neurons (BackEISNN). The experimental results on several standard datasets have shown that the two modules not only accelerate the convergence of the network but also improve the accuracy. For the MNIST, FashionMNIST, and N-MNIST datasets, our model has achieved state-of-the-art performance. For the CIFAR10 dataset, our BackEISNN also gets remarkable performance on a relatively light structure that competes against state-of-the-art SNNs.

Index Terms—SNNs, Adaptive Self-Feedback Connections, Dynamic Balanced Excitatory-Inhibitory Neurons, Brain-Inspired

I. INTRODUCTION

In the past few years, deep neural networks (DNNs) have made tremendous progress in various machine learning tasks, such as computer vision [1], natural language processing [2], and speech recognition [3]. However, DNNs only mimic the hierarchical topology structure of the information flow in the brain and process data in a real-valued form, far from the information-processing mechanisms in the brain. The spikes play a crucial role in efficient information processing. As a result, SNNs are developed to emulate the information processing in the brain. SNNs are considered the third-generation neural network [4], the discrete spike communication between

the spiking neurons, multiple brain-inspired learning rules, and the intricate connections make it more biologically plausible and energy-efficient.

However, due to the lack of an effective training algorithm, the development of SNNs has stalled for a long time and has not yet demonstrated comparable performance to DNNs. Many researchers took inspiration from synapse learning in the brain, thus introduce some mechanisms that existed in the brains such as Spike-Timing-Dependent Plasticity (STDP) [5], Short-Term Facilitation (STF) or Depression (STD) into learning the weight of the SNNs [6], [7], [8], [9], [10], [11]. Although it has strong biological interpretability, most of these mechanisms are local learning rules, as the number of network layers goes more in-depth, it is difficult to achieve global convergence. Although GLSNN [12] introduced global feedback layers combined with local optimization learning rules, which alleviated this problem to a certain extent, it still performs poorly on complex datasets.

The success of deep learning comes from the proposal of the backpropagation (BP) algorithm. However, the discontinuous and non-differentiable characteristic of SNNs have impeded the BP implementation based on gradient descent. It's not feasible to apply the BP algorithm to the training of SNNs directly. An alternative method is to convert well-trained DNNs to SNNs through additional adjustments to parameters [13], [14], [15], [16]. The conversion methods have achieved state-of-the-art accuracy on large datasets like ImageNet and complex architectures, such as VGG and ResNet. However, the superior performance comes from the well-trained DNNs, which does not solve the problem of SNNs' training. Also, the DNN-based training does not take full advantage of the temporal information in SNNs. When the SNNs go more in depth, the simulation length should be large enough to make the mean firing rates close to the real value of DNNs. Recently, due to the proposal of the approximation of the gradient of the spiking threshold functions, the backpropagation algorithm can be directly applied to the training of SNNs [17], [18], [19], [20]. In this process, the discontinuous derivative of the spiking neurons is approximated by a continuous function. Although they perform well on some simple datasets, there still exists a particular gap between them and the traditional DNNs.

In addition to the typical spiking neurons and the feedforward network structures, there are many other complicated mechanisms to support the brain's learning and inference. Here, we draw some mechanisms from the brain to further improve the BP-based SNNs. First, the typical network struc-

Dongcheng Zhao and Yang Li are with the Research Center for Brain-Inspired Intelligence, Institute of Automation, Chinese Academy of Sciences, Beijing 100190, China, and also with the School of Artificial Intelligence, University of Chinese Academy of Sciences, Beijing 100049, China, (e-mail: zhaodongcheng2016@ia.ac.cn)

Yi Zeng is with the Research Center for Brain-Inspired Intelligence, Institute of Automation, Chinese Academy of Sciences, Beijing 100190, China, also with the University of Chinese Academy of Sciences, Beijing 100049, and also with the Center for Excellence in Brain Science and Intelligence Technology, Chinese Academy of Sciences, Shanghai 200031, China (e-mail: yi.zeng@ia.ac.cn)

The corresponding author is Yi Zeng.

ture is based on simple forward structures. When the spiking neuron’s membrane reaches the threshold, it releases a spike to the postsynaptic neuron. However, there are many other complex structures in the brain, such as the feedback connections [21], [22]. The cross-layer feedback connections bring the information predicted by the higher cortex to the early cortical areas to help the inference and learning. Specially, the autapse connected to the soma [23], [24], [25] applies the time-delayed feedback on the neuron’s membrane potential to regulate the spike precision and network activity.

As well, the excitatory spiking neurons are used in most of the current spiking neural networks. After the presynaptic neuron’s membrane potential reaches the threshold, it releases the spike, increasing the membrane potential which makes the postsynaptic neurons easier fire. However, there exist both excitatory and inhibitory neurons in the brain. The dynamic balance between excitatory and inhibitory neurons is crucial to healthy cognition and behavior [26], [27].

Taking inspiration from the two mechanisms, we introduce an adaptive time-delayed self-feedback mechanism to help regulate the membrane potential, which has improved the performance of the BP-based SNNs to some extent. Also, we introduce the inhibitory neurons in the BP-based SNNs. The dynamic balance of the excitatory and inhibitory neurons mechanism has accelerated the convergence of the neural networks and has improved the networks’ performance. With the combination of the two mechanisms, we propose a deep spiking neural network with adaptive self-feedback and balanced excitatory inhibitory neurons (BackEISNN). And we have conducted experiments on several commonly used datasets to verify the performance of our BackEISNN. It has achieved state-of-the-art performance on MNIST, NMNIST, FashionMNIST datasets. Our contribution can be summarized as follows:

- We introduce the adaptive self-feedback mechanism (SFBM) to apply the time-delayed feedback on the membrane potential of the spiking neurons to regulate the spike precision.
- We introduce the balanced excitatory and inhibitory neurons mechanism (BEIM) to control the spikes firing in a balanced form, which has made the network achieve faster convergence and better performance.
- Combined with the SFBM and BEIM, we have conducted extensive experiments on MNIST, Fashion-MNIST, NMNIST, CIFAR10 datasets. The results indicate that the proposed mechanisms could significantly improve the performance of the BP-based SNNs and accelerate the training of SNNs. We have achieved state-of-the-art performance on MNIST, NMNIST, and FashionMNIST datasets. And for the CIFAR10 dataset, we also get remarkable performance on a relatively light structure.

II. RELATED WORK

This section will review several BP-based SNNs in recent years and those which introduced some biological mechanism for better training.

The spikeprop [28] algorithm could be viewed as the first attempt to train SNNs by operating on discontinuous spike activities. However, the single spike output restriction had limited it to demonstrate competitive performance on real-world tasks. DSN [29] proposed a spiking version of backpropagation to train a deep SNN with relu units. SCSNN [30] treated the spike count as the surrogate for gradient backpropagation. BP-SNN [17] treated the membrane potentials of spiking neurons as differentiable signals and treated spiking times as noise.

However, all these methods lack explicit consideration of the temporal correlation of neural activities. To tackle the problems mentioned above, Slayer [31] handled the non-differentiable problem of the spike function by considering the temporal dependency between input and output signals. STBP [20] proposed spatial-temporal backpropagation for training SNNs, and the improved version [18] introduced NeuNorm and decoding voting mechanisms, achieving higher performance on various datasets. HM2-BP [19] proposed hybrid macro/micro level backpropagation. The micro-level was used to capture the temporal effects; both the macro and micro levels were used to compute the rate-coded errors. ST-RSBP [32] presented a spike-train level backpropagation algorithm to help train a recurrent spiking neural network. LSNN [33] introduced the adaptive neurons in the recurrent spiking neural networks to support the network acquire knowledge in a learning-to-learn scheme. TSSL-BP [34] introduced two types of inter-neuron and intra-neuron dependencies of error backpropagation to improve the temporal learning precision. The performance of the BP-based SNNs are still far behind that of DNNs due to the special spike transmission form.

Others took inspiration from the learning of the brains from the structures and learning rules to further improve the learning. LISNN [35] introduced lateral interaction in SNNs, which enhanced the performance of the network and its robustness to noise to a certain extent. However, the performance was only verified on simple datasets. In addition to the STDP learning rules, Balance SNN [11] introduced the Short Term Plasticity (STP), and balance of excitatory-inhibitory neurons based on VPSNN [10], but the proportion of excitability here was tested by manually trying different ratios. Also, winner-takes-all (WTA) [8], population coding [36] were introduced into training SNNs. The performance gap still exists compared with the DNNs due to the special spike transmission form, which shows that we should take more inspiration from the brain’s learning. Here, inspired by the autapse and the balanced excitatory and inhibitory neurons, we introduce the adaptive self-feedback mechanism and the balanced excitatory and inhibitory neurons mechanism to help BP-based SNNs achieve better performance.

III. METHODS

In this section, we will first give an introduction to the basic neuron model we used. And we will provide a detailed description of our SFBM and the BEIM. Finally, the whole pipeline of our BackEISNN will be presented.

A. Basic LIF Neuron Model

Leaky-Integrate-and-Fire (LIF) model is the most commonly used to describe the dynamic neural activities of the spiking neurons, including the dynamic changes of membrane potential and the firing process of spikes, which can be formulated as a differential Eq. 1:

$$\tau \frac{dV(t)}{dt} = -V(t) + RI(t) \quad (1)$$

$V(t)$ is the membrane potential, R is the membrane resistance, and $\tau = CR$ denotes the time constant. $I(t) = \sum_j^N w_{j,i} \delta_j$ denotes the total input generated by synaptic currents triggered by the arrival of spikes of presynaptic neurons. And when the membrane potential reaches the threshold V_{th} , the neuron will fire a spike.

For a better computational model, we modify Eq. 1 in discrete form as shown in Eq. 2:

$$V_t = (1 - \frac{1}{\tau})V_{t-1} + \frac{1}{C}I_t \quad (2)$$

When the potentials fire a spike the membrane potential will be reset to V_{reset} . By assuming $V_{reset} = 0$, $C = 1$ as usual, the final equation can be written as:

$$V_t = (1 - \frac{1}{\tau})V_t(1 - \delta_{t-1}) + I_t \quad (3)$$

δ_{t-1} is the spikes at time $t-1$. When performing backpropagation in SNNs, the spike activation cannot be derived, which is a key issue that restricts the development of BP-trained SNNs. Here, we use the gradient of the rectangular function $S(V)$ to replace that of the original hard threshold function, which is also used in [18], [20], the derivative of the rectangular function is shown in Eq. 4:

$$\frac{\partial S(V)}{\partial V} = \begin{cases} 1 & \text{if } \frac{-1}{2} \leq V - V_{th} \leq \frac{1}{2} \\ 0 & \text{else} \end{cases} \quad (4)$$

B. Adaptive Self-Feedback Mechanism

In the brain, in addition to the traditional way of information transmission, presynaptic neuron emits spikes along the axons to the postsynaptic neurons. Specially, the autapse that connects the soma with a self-feedback loop that transmit information to itself. As shown in Fig. 1, the autapses in the brain act on the membrane potential to help regulate the spike precision and network activity in a time-delayed self-feedback.

Inspired by the brain's autapses, we have introduced an adaptive self-feedback mechanism on the convolutional spiking neural networks. To reflect the modeling of the time-delay, we use the spikes fired at the last moment to regulate the input of the neurons.

As shown in Fig. 1, the spikes sent by the layer at the last moment were put into the convolution operation with a sigmoid activation function, which takes more advantage of the temporal information of SNNs. The output size is the same as the input current received by the layer, and the value is between 0 and 1. As a result, it can adjust the input adaptively

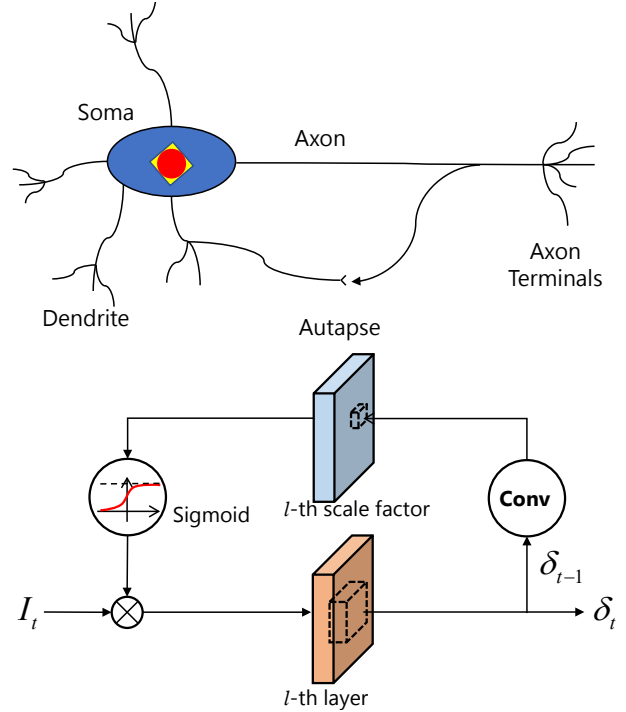


Fig. 1. The top is autapse in the brain, which connects the soma with a self-feedback manner. The bottom is the corresponding computational model.

to control the input to the membrane potential so that the spikes will fire more accurately.

The detailed description of the adaptive self-feedback mechanism is shown in Eq. 5, f denotes the convolution operation, σ denotes the sigmoid function, the self-feedback gate SFB_t is multiplied to the input. \odot means the element-wise.

$$\begin{cases} SFB_t = \sigma(f(\delta_{t-1})) \\ V_t = (1 - \frac{1}{\tau})V_{t-1}(1 - \delta_{t-1}) + SFB_t \odot I_t \end{cases} \quad (5)$$

C. Balanced Excitatory and Inhibitory Neurons Mechanism

There exist both excitatory and inhibitory neurons in the brain. The balanced combination of them helps the learning and inference. As can be seen in Fig. 3, the excitatory neurons exhibit the excitatory postsynaptic potential (EPSP), which allows the postsynaptic neuron easier to fire. In contrast, the inhibitory neurons exhibit the inhibitory postsynaptic potential (IPSP), making the postsynaptic neuron less likely to fire. We define excitatory neurons that release the positive spikes and inhibitory neurons that release negative spikes to simplify excitatory and inhibitory neurons' modeling.

The positive combined with negative spikes were first used in SpikeGrad [37], which can be seen in Eq. 6:

$$S(V) = \begin{cases} 1 & \text{if } V \geq V_{th} \\ -1 & \text{if } V \leq -V_{th} \\ 0 & \text{else} \end{cases} \quad (6)$$

The rules for sending positive or negative spikes are determined in advance. A positive spike occurs when the membrane potential exceeds the positive threshold, and a negative spike

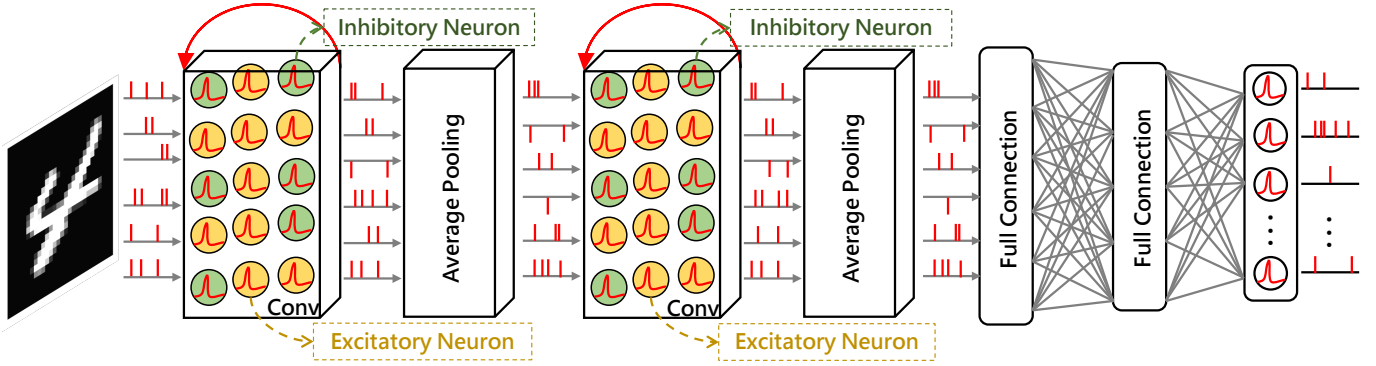


Fig. 2. The whole pipeline of our BackEISNN. The adaptive self-feedback mechanism is used to control the membrane to spike more precisely. The balanced excitatory and inhibitory mechanism is used to help the layer release spikes in a balanced manner.

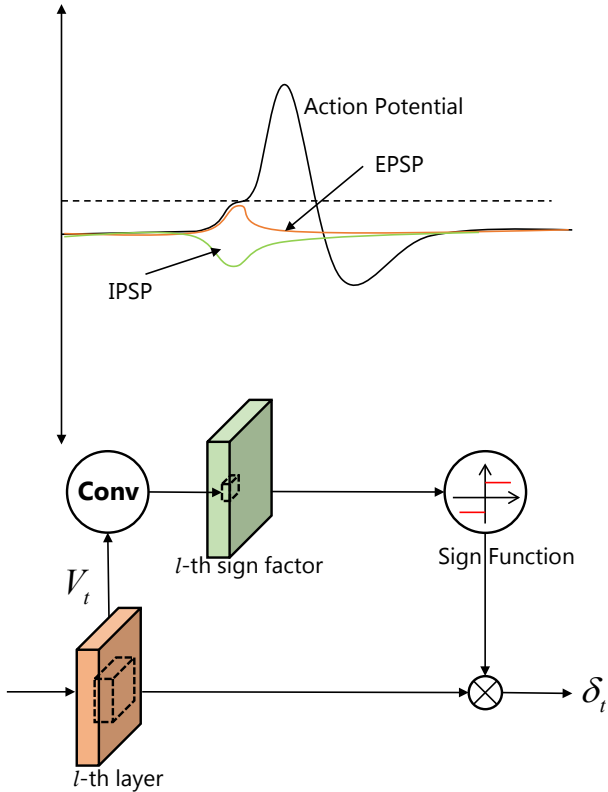


Fig. 3. The balance of the excitatory and inhibitory neurons in the brain and the corresponding computational model.

occurs when the membrane is below the negative threshold. While in the biological brain, the neuron would not fire a spike when the membrane potential does not reach the threshold. In this paper, we introduce a mechanism to determine whether the neurons are excitatory dynamically. Inspired by Zhu’s work [38] that the balance of excitation and inhibition is achieved at different membrane potentials of cortical neurons, we use the membrane potential to guide the generation of the balance.

As shown in Fig. 3, before the membrane potential is sent to the threshold function, it is sent into a convolutional layer with a sign activation function to determine whether the neurons are excitatory. And the gradient of this challenging

function is processed the same as the hard threshold function mentioned above. When we get the neuron’s positive and negative attributes, and the membrane potential reaches the threshold, we can decide whether to send a positive or negative spike.

The details can be seen in the Eq. 7, f denotes the convolution operation, θ denotes the sign function, the excitatory and inhibitory neuron determining gate EI_t is multiplied to the output.

$$\begin{cases} EI_t = \theta(f(V_t)) \\ \delta_t = EI_t \odot S(V_t) \end{cases} \quad (7)$$

D. The Whole BackEISNN Model

The whole training process is shown in Fig. 2. The input was sent into the spiking convolutional networks and combined the two mechanisms mentioned above. The whole update process of the LIF neuron is shown in Eq. 8:

$$\begin{cases} SFB_t = \sigma(f(\delta_{t-1})) \\ V_t = (1 - \frac{1}{\tau})V_{t-1}(1 - \delta_{t-1}) + SFB_t \odot I_t \\ EI_t = \theta(f(V_t)) \\ \delta_t = EI_t \odot S(V_t) \end{cases} \quad (8)$$

Assuming that the output of the last layer is O_t at time t , and for a given time window T , the mean average firing rates is $1/T \sum_{t=1}^T O_t$, y_s is the true label, here we use the Mean Square Error loss function, as can be seen in Eq. 9.

$$L = \frac{1}{S} \sum_{s=1}^S \|y_s - 1/T \sum_{t=1}^T O_t\|_2^2 \quad (9)$$

IV. EXPERIMENTS

In this section, we perform the experiments on TITAN A100 GPU with PyTorch framework [39]. We initialize the network weight with the default method of PyTorch. The optimizer is the Adam [40] optimizer. The batch size is set to 100. The epochs are set with 200. The learning rate lr is set with 0.001 and decayed to $0.1lr$ every 40 epochs. We set $V_{th} = 0.5$. To illustrate the above two modules’ improvement on the representation learning ability, we only apply the above two modules in the convolutional layers. We conducted the experiments on MNIST [41], N-MNIST [42], Fashion MNIST [43], and CIFAR10 [44] datasets to illustrate the superiority of our proposed BackEISNN model.

A. MNIST

MNIST dataset is the most widely used classification dataset to measure the performance of deep learning models. It consists of 60,000 training examples and 10,000 test samples, describing the hand-written digits from 0 to 9. The shape of the sample is 28*28. For the static MNIST dataset, we first convert the samples into spike trains. The normalized pixel is converted to 1 or 0, comparing the pixel value with a random number between 0 to 1. If the value is greater than the random number, then a spike is triggered. Our network structure is the same with ST-RSBP [32], which used two convolutional layers and two linear layers. However, in our experiment, we did not use the data argumentation method elastic distortion. First, we fixed the simulation time to 20 and explored the impact of different kernel sizes of the two separate modules on the network results.

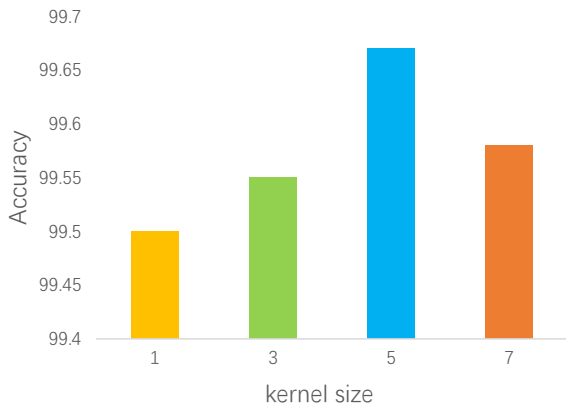


Fig. 4. The test accuracy on MNIST with different kernel size of the two modules.

As shown in Fig. 4, when the kernel size is set with 5, the network achieves the best performance. Then we explore the impact of different simulation lengths on the network performance with the kernel size fixed at 5.

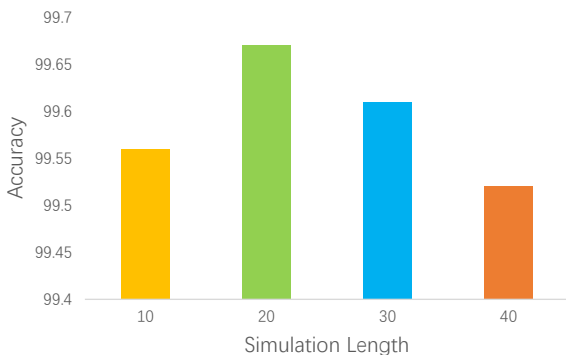


Fig. 5. The test accuracy on MNIST with different simulation length.

As shown in Fig. 5, when the simulation time is set with 10, the network performance has reached 99.56%, which has achieved relatively high performance when the simulation length is short. And when the simulation length is set with 20, the network reaches the best performance.

We have set the kernel size with 5 and the simulation length with 20. The experiment was repeated five times with different random number seeds. And the test accuracy is shown in Fig. 6. Each category is well classified.

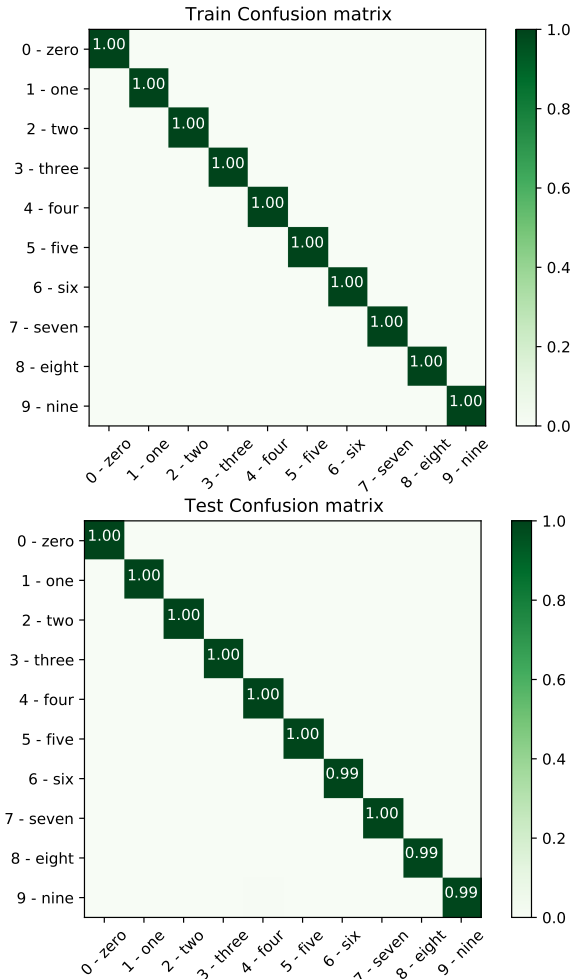


Fig. 6. Confusion matrix of the BackEISNN on the MNIST dataset. The top is the training dataset, and the bottom is the test dataset.

As shown in the Tab. I, several other BP-based SNNs were compared with our BackEISNN. Compared with STBP, which does not introduce the SFBM and the BEIM, we have an improvement of 0.25%. For other BP-based SNN frameworks, our EILoopSNN has exceeded all of them, which is the state-of-the-art for the MNIST dataset.

TABLE I
PERFORMANCES OF BP BASED SNNs ON MNIST

Model	Structure	Mean	Stddev	Best
Spiking CNN [17]	20C5-P2-50C5-P2-200	-	-	99.31
SLAYER [31]	12C5-P2-64C5-p2	99.36	0.05	99.41
STBP [20]	15C5-P2-40C5-p2-300	-	-	99.42
HM2BP [19]	15C5-P2-40C5-p2-300	99.42	0.11	99.49
LISNN [35]	32C3-P2-32C3-P2-128	-	-	99.5
TSSL-BP [34]	15C5-P2-40C5-p2-300	99.5	0.02	99.53
ST-RSBP [32]	15C5-P2-40C5-p2-300	99.57	0.04	99.62
BackEISNN (ours)	15C5-P2-40C5-p2-300	99.58	0.06	99.67

B. N-MNIST

The N-MNIST dataset is a neuromorphic version of the MNIST dataset by mounting a Dynamic Version Sensor (DVS) in front of static digit images on a computer screen. It has 60,000 training samples and 10,000 test samples, which is the same as MNIST. The DVS is moved in the direction of three sides of the isosceles triangle in turn and collects the two-channel spike event (since the intensity can be increased or decreased) triggered by the pixel change lasting for 300ms. Due to each image’s relative shifts, each sample of the N-MNSIT is a spatial-temporal pattern with 34x34x2 spike sequences. Since the time resolution is 1us, there is a total of 300,000-time steps. To speed up the simulation, we reduced it to 100-time steps, which means no matter how many events during the 3000-time intervals, we only record one spike. We also test the influence of different kernel sizes, and as shown in Tab. II, when the kernel size is set with 3, the network reaches the highest performance.

TABLE II
THE PERFORMANCE OF NETWORK ON N-MNSIT DATASET WITH DIFFERENT KERNEL SIZES

kernel size	kernel 1	kernel 3	kernel 5	kernel 7
performance	99.44	99.57	98.89	96.55

The experiment is first conducted on 100-time steps. As can be seen in Tab. III, our BackEISNN-100 has achieved 99.57% accuracy and has achieved state-of-the-art performance compared with other BP-based SNNs. Moreover, we use the first 30 time-steps to experiment, and the result is denoted as BackEISNN-30, which still keeps the high level of performance.

TABLE III
PERFORMANCES OF BP BASED SNNs ON N-MNIST

Model	Structure	Mean	Stddev	Best
HM2-BP [19]	400-400	-	-	98.88
SLAYER [31]	Net 1	-	-	99.2
TSSL-BP 30 [34]	Net 1	99.23	0.05	99.28
TSSL-BP 100 [34]	Net 1	99.35	0.03	99.4
STBP [18]	Net 2	-	-	99.44
LISNN [35]	Net 3	-	-	99.45
STBP NeuNorm [18]	Net 2	-	-	99.53
BackEISNN-30 (Ours)	Net 1	99.47	0.05	99.56
BackEISNN-100 (Ours)	Net 1	99.5	0.06	99.57

¹ Net 1 is 12C5-P2-64C5-P2

² Net 2 is 128C3-128C3-P2-128C3-256C3-P2-1024-Voting

³ Net 3 is 32C3-P2-32C3-P2-128

C. FashionMNIST

Fashion-MNIST is a complicated version compared to MNIST. It consists of gray-scale images of clothing experiments. As the same as the MNIST dataset process, the dataset is processed to spike trains.

First, we also analyze the impact of different kernel sizes on performance. As shown in the Tab IV, when the kernel size is set with 5, the network gets the best performance.

Then, with the kernel size fixed at 5, we analyze the influence of the simulation length. As can be seen in the Tab V,

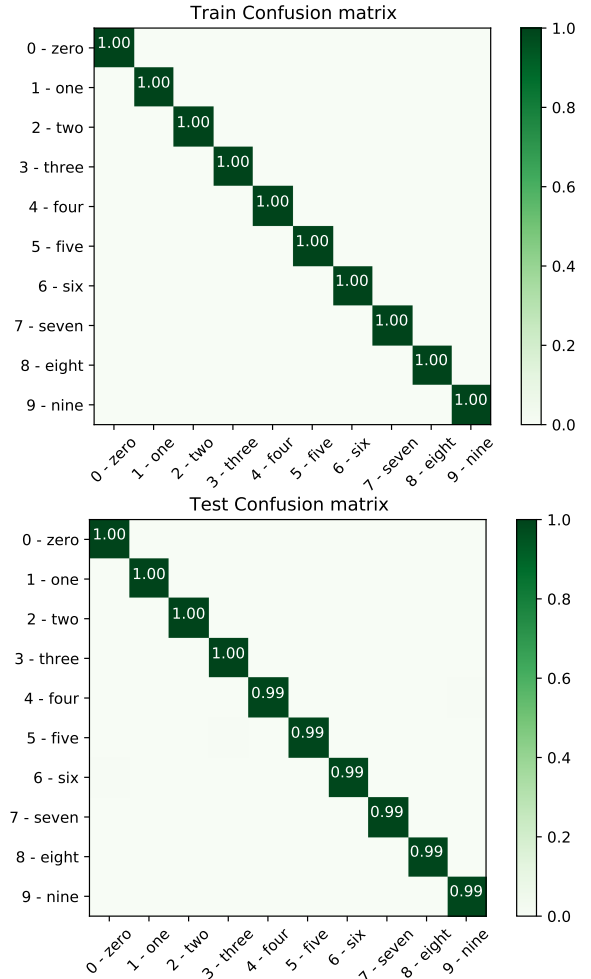


Fig. 7. Confusion matrix of the BackEISNN on the N-MNIST dataset. The top is the training dataset, and the bottom is the test dataset.

TABLE IV
THE PERFORMANCE OF NETWORK ON FASHIONMNSIT DATASET WITH DIFFERENT KERNEL SIZES IN ENCODING MANNER.

kernel size	kernel 1	kernel 3	kernel 5	kernel 7
performance	92.32	92.49	92.51	92.36

when the simulation length is 30, our BackEISNN reaches the best performance.

TABLE V
THE PERFORMANCE OF NETWORK ON FASHIONMNSIT DATASET WITH DIFFERENT SIMULATION LENGTH IN ENCODING MANNER.

simulation length	10	20	30	40
performance	92.13	92.51	92.7	92.2

For the TSSL-BP model, the real-value was directly inputted into the network. To be consistent with this approach, we also use the real-valued input current as of the direct input of the network to demonstrate the influence of the kernel size and the simulation length. We repeat the experiment as mentioned above. As shown in Tab. VI and Tab. VII when the kernel size is 3 and the simulation length is 20, the network reaches the highest performance.

TABLE VI

THE PERFORMANCE OF NETWORK ON FASHIONMNSIT DATASET WITH DIFFERENT KERNEL SIZES IN DIRECT INPUT MANNER.

kernel size	kernel 1	kernel 3	kernel 5	kernel 7
performance	92.77	93.45	93.12	92.37

TABLE VII

THE PERFORMANCE OF NETWORK ON FASHIONMNSIT DATASET WITH DIFFERENT SIMULATION LENGTH IN DIRECT INPUT MANNER.

simulation length	10	20	30	40
performance	92.86	93.45	93.35	93.11

We repeat the experiments five times with the parameters mentioned above. The result of the encoding input is denoted as BackEISNN-E, while the direct input is denoted as BackEISNN-D. As shown in Tab. VIII, for the encoding results, our BackEISNN-E has achieved 92.7% accuracy and surpasses most of the results. For the TSSL-BP, it uses the direct input encoding, as shown in Tab. VIII, our BackEISNN-D has achieved state-of-the-art performance on the FashionM-NIST dataset, indicating our algorithm’s progressive nature.

TABLE VIII

PERFORMANCES OF BP BASED SNNs ON FASHIONMNIST

Model	Structure	Mean	Stddev	Best
HM2BP [19]	400-400	-	-	88.99
GLSNN [12]	256*8	-	-	89.02
ST-RSBP [32]	400-R400	-	-	90.13
LISNN [35]	Net 1	-	-	92.07
BackEISNN-E (ours)	Net 2	92.56	0.08	92.7
TSSL-BP [34]	Net 2	92.69	0.09	92.83
BackEISNN-D (Ours)	Net 2	93.04	0.31	93.45

¹ Net 1 is 32C3-P2-32C3-P2-128

² Net 2 is 32C5-P2-64C5-p2-1024

To better analyze the result, we plot the confusion matrix. As can be seen in Fig 8, for the training dataset, our BackEISNN can distinguish each category clearly. However, for the test dataset, the main problem is that we cannot determine the T-shirt and Shirt well, as they look very similar, and for humans, they can not distinguish them well.

D. CIFAR10

Furthermore, we apply our BackEISNN to the CIFAR10 dataset. Compared to MNIST and FashionMNSIT, CIFAR10 is a more challenging color image dataset with an image size of 32*32*3. It has 60,000 color images belong to 10 classes, and 50,000 for the train, 10,000 for the test. The dataset is normalized, random cropping, and horizontal flipping for data augmentation, commonly used for CIFAR10 preprocessing. We also used Dropout after each layer, which is also adopted in STBP and TSSL-BP. The network structure is 128C3-P2-256C3-P2-512C3-P2-1024. And the kernel size for the two modules is set with 3. The simulation length is charged with 20.

As can be seen in Tab IX, the accuracy of our BackEISNN has reached 90.93 %, which exceeds the SNNs trained with BP, decode Voting, and NeuNorm. For the TSSL-BP method, the

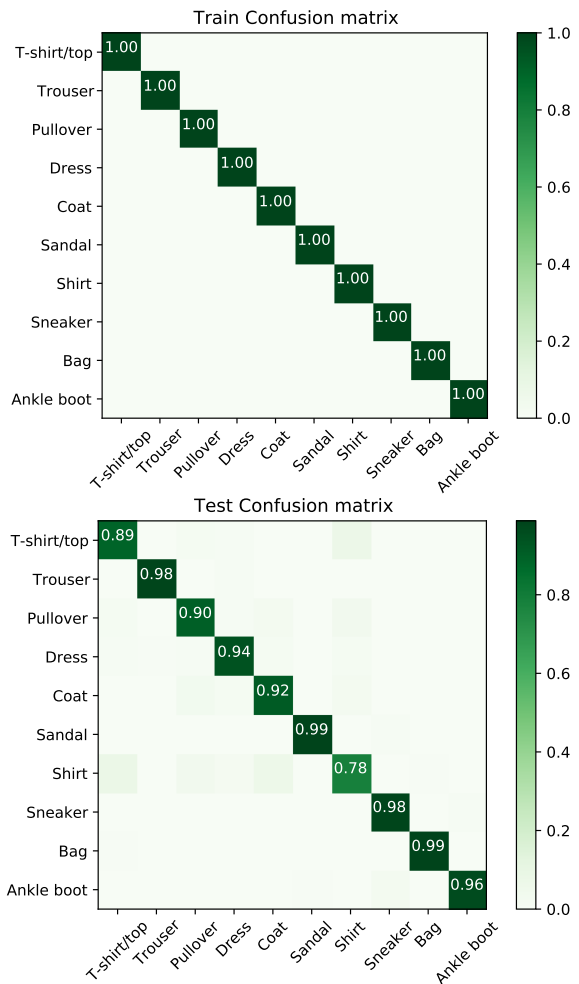


Fig. 8. Confusion matrix of the BackEISNN on the FashionMNIST dataset. The top is the training dataset, and the bottom is the test dataset.

warm-up mechanism is used that when very low firing activity levels are observed, the network will use the continuous sigmoid function of membrane potential to approximate the activation so that the errors can be propagated back when there is no spike for a deeper spiking neural network. And the warm-up mechanism is not adopted in our experiment. Also, our experiment uses a relatively light structure with three convolutional layers and two linear layers. In contrast, for the TSSL-BP and STBP, the deep network with five convolutional layers is used.

TABLE IX
PERFORMANCES OF BP BASED SNNs ON CIFAR10

Model	Method	Performance
STBP [18]	BP and Decode Voting	89.83
STBP [18]	BP, Decode Voting and NeuNorm	90.53
BackEISNN (Ours)	BP, SFBM and BEIM	90.93
TSSL-BP [34]	Inter-neuron BP and Intra-neuron BP	91.41

V. DISCUSSION

To further illustrate the contributions of different modules of our algorithm, we conducted ablation studies on the CIFAR10

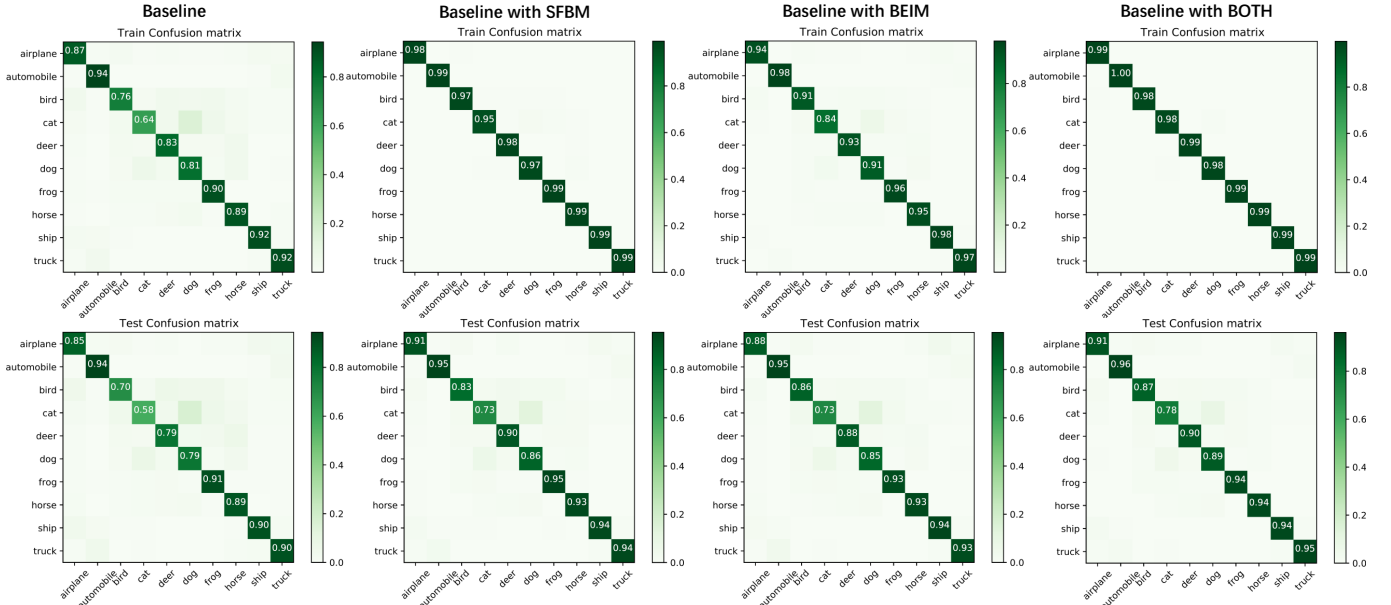


Fig. 9. Confusion matrix of the BP-based SNN with the SFBM, BEIM, and both of them on the CIFAR10 dataset. The top is the training dataset, and the bottom is the test dataset.

experiment. The network structure is the same as mentioned above. As can be seen in Tab X, for the baseline without SFBM and BEIM, the accuracy is only 82.6%. With the introduction of SFBM, the accuracy increases to 88.86%, and with the introduction of BEIM, the accuracy rises to 89.32%. With both of the mechanisms introduced, our BackEISNN has reached 90.93% accuracy, which shows that the combination of the two mechanisms has better improved the network’s performance.

TABLE X
ABLATION STUDIES OF BACKEISNN ON CIFAR10

Model	With SFBM	With BEIM	Performance
Baseline	-	-	82.6
Baseline	✓	-	88.86
Baseline	-	✓	89.32
Baseline	✓	✓	90.93

We also plot the baseline’s test accuracy, baseline with SFBM, baseline with BEIM, baseline with Both. As can be seen in Fig 10, with the introduction of two mechanisms, our network has not only higher accuracy but also a faster convergence rate.

To better illustrate the two modules’ superiority, we plot the confusion matrix of the four models. As shown in Fig 9, for the original model without SFBM and BEIM module, for the similar object, such as airplane and bird, the cat and dog, the horse and deer, the networks would be confused to distinguish them clearly. However, when the two modules are introduced, the networks would distinguish them more clearly. For the other not confused categories, the BackEISNN also improves the accuracy. That’s to say, with the introduction of the adaptive self-feedback module and the dynamic balance excitatory and inhibitory neurons, the network not only improves the accuracy of the easily classified categories but also improves

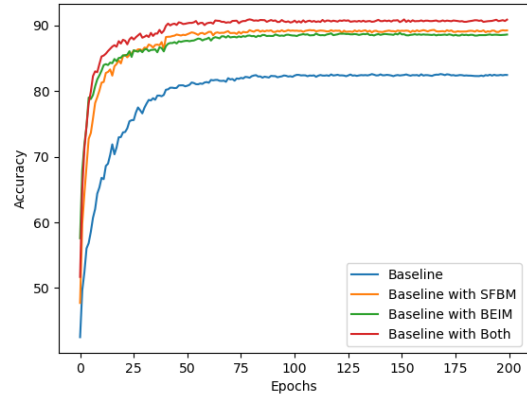


Fig. 10. The test accuracy on CIFAR10 dataset with and without SFBM and BEIM.

the classification accuracy of the easily confused categories to a large extent.

VI. CONCLUSION

There is still a performance gap between the BP-based SNNs and DNNs due to the particular data transmission mode in the SNNs, indicating that only BP is not enough for the training. In this paper, inspired by the autapses, which connect the soma in a self-feedback manner, we propose to apply the time-delayed feedback on the neuron’s membrane potential. The input current is gated with the spikes’ information at the last moment to regulate the spike precision and the temporal information. Also, we adopt the balanced excitatory and inhibitory neuron mechanism to control the output form of the spiking neurons dynamically. The introduction of the two mechanisms into the spiking neural networks trained with BP

accelerates the convergence of the network and improves the accuracy. For the MNIST, FashionMNIST, and N-MNIST, our BackEISNN has achieved state-of-the-art performance. For the CIFAR10 dataset, our BackEISNN also gets remarkable performance in a relatively light structure that competes against state-of-the-art SNNs.

ACKNOWLEDGEMENT

This work is supported by the National Key Research and Development Program (2020AAA0104305), the Strategic Priority Research Program of the Chinese Academy of Sciences (Grant No. XDB32070100), the Beijing Municipal Commission of Science and Technology (Grant No. Z181100001518006), and the Beijing Academy of Artificial Intelligence (BAAI).

REFERENCES

- [1] A. Krizhevsky, I. Sutskever, and G. E. Hinton, "Imagenet classification with deep convolutional neural networks," *Communications of the ACM*, vol. 60, no. 6, pp. 84–90, 2017.
- [2] R. Collobert and J. Weston, "A unified architecture for natural language processing: Deep neural networks with multitask learning," in *Proceedings of the 25th international conference on Machine learning*, 2008, pp. 160–167.
- [3] D. Amodei, S. Ananthanarayanan, R. Anubhai, J. Bai, E. Battenberg, C. Case, J. Casper, B. Catanzaro, Q. Cheng, G. Chen *et al.*, "Deep speech 2: End-to-end speech recognition in english and mandarin," in *International conference on machine learning*. PMLR, 2016, pp. 173–182.
- [4] W. Maass, "Networks of spiking neurons: the third generation of neural network models," *Neural networks*, vol. 10, no. 9, pp. 1659–1671, 1997.
- [5] G.-q. Bi and M.-m. Poo, "Synaptic modifications in cultured hippocampal neurons: dependence on spike timing, synaptic strength, and postsynaptic cell type," *Journal of neuroscience*, vol. 18, no. 24, pp. 10464–10472, 1998.
- [6] A. Tavanaei and A. S. Maida, "Bio-inspired spiking convolutional neural network using layer-wise sparse coding and stdp learning," *arXiv preprint arXiv:1611.03000*, 2016.
- [7] —, "Multi-layer unsupervised learning in a spiking convolutional neural network," in *2017 International Joint Conference on Neural Networks (IJCNN)*. IEEE, 2017, pp. 2023–2030.
- [8] P. U. Diehl and M. Cook, "Unsupervised learning of digit recognition using spike-timing-dependent plasticity," *Frontiers in computational neuroscience*, vol. 9, p. 99, 2015.
- [9] P. Falez, P. Tirilly, I. M. Bilasco, P. Devienne, and P. Boulet, "Multi-layered spiking neural network with target timestamp threshold adaptation and stdp," *arXiv preprint arXiv:1904.01908*, 2019.
- [10] T. Zhang, Y. Zeng, D. Zhao, and M. Shi, "A plasticity-centric approach to train the non-differential spiking neural networks," in *Thirty-Second AAAI Conference on Artificial Intelligence*, 2018.
- [11] T. Zhang, Y. Zeng, D. Zhao, and B. Xu, "Brain-inspired balanced tuning for spiking neural networks," in *IJCAI*, 2018, pp. 1653–1659.
- [12] D. Zhao, Y. Zeng, T. Zhang, M. Shi, and F. Zhao, "Glsnn: A multi-layer spiking neural network based on global feedback alignment and local stdp plasticity," *Frontiers in Computational Neuroscience*, vol. 14, 2020.
- [13] P. U. Diehl, D. Neil, J. Binas, M. Cook, S.-C. Liu, and M. Pfeiffer, "Fast-classifying, high-accuracy spiking deep networks through weight and threshold balancing," in *2015 International Joint Conference on Neural Networks (IJCNN)*. IEEE, 2015, pp. 1–8.
- [14] Q. Xu, Y. Qi, H. Yu, J. Shen, H. Tang, and G. Pan, "Csn: An augmented spiking based framework with perceptron-inception," in *IJCAI*, 2018, pp. 1646–1652.
- [15] A. Sengupta, Y. Ye, R. Wang, C. Liu, and K. Roy, "Going deeper in spiking neural networks: Vgg and residual architectures," *Frontiers in neuroscience*, vol. 13, 2019.
- [16] Y. Hu, H. Tang, Y. Wang, and G. Pan, "Spiking deep residual network," *ArXiv*, vol. abs/1805.01352, 2018.
- [17] J. H. Lee, T. Delbruck, and M. Pfeiffer, "Training deep spiking neural networks using backpropagation," *Frontiers in neuroscience*, vol. 10, p. 508, 2016.
- [18] Y. Wu, L. Deng, G. Li, J. Zhu, Y. Xie, and L. Shi, "Direct training for spiking neural networks: Faster, larger, better," in *Proceedings of the AAAI Conference on Artificial Intelligence*, vol. 33, 2019, pp. 1311–1318.
- [19] Y. Jin, W. Zhang, and P. Li, "Hybrid macro/micro level backpropagation for training deep spiking neural networks," in *Advances in Neural Information Processing Systems*, 2018, pp. 7005–7015.
- [20] Y. Wu, L. Deng, G. Li, J. Zhu, and L. Shi, "Spatio-temporal backpropagation for training high-performance spiking neural networks," *Frontiers in neuroscience*, vol. 12, 2018.
- [21] D. J. Felleman and D. E. Van, "Distributed hierarchical processing in the primate cerebral cortex," *Cerebral cortex (New York, NY: 1991)*, vol. 1, no. 1, pp. 1–47, 1991.
- [22] O. Sporns and J. D. Zwi, "The small world of the cerebral cortex," *Neuroinformatics*, vol. 2, no. 2, pp. 145–162, 2004.
- [23] K. Ikeda and J. M. Bekkers, "Autapses," *Current Biology*, vol. 16, no. 9, p. R308, 2006.
- [24] C. Wang, S. Guo, Y. Xu, J. Ma, J. Tang, F. Alzahrani, and A. Hobiny, "Formation of autapse connected to neuron and its biological function," *Complexity*, vol. 2017, 2017.
- [25] L. Yin, R. Zheng, W. Ke, Q. He, Y. Zhang, J. Li, B. Wang, Z. Mi, Y.-s. Long, M. J. Rasch *et al.*, "Autapses enhance bursting and coincidence detection in neocortical pyramidal cells," *Nature communications*, vol. 9, no. 1, pp. 1–12, 2018.
- [26] R. Rubin, L. Abbott, and H. Sompolinsky, "Balanced excitation and inhibition are required for high-capacity, noise-robust neuronal selectivity," *Proceedings of the National Academy of Sciences*, vol. 114, no. 44, pp. E9366–E9375, 2017.
- [27] N. Dehghani, A. Peyrache, B. Telenczuk, M. Le Van Quyen, E. Hålgren, S. S. Cash, N. G. Hatsopoulos, and A. Destexhe, "Dynamic balance of excitation and inhibition in human and monkey neocortex," *Scientific reports*, vol. 6, no. 1, pp. 1–12, 2016.
- [28] S. M. Bohte, J. N. Kok, and J. A. La Poutré, "Spikeprop: backpropagation for networks of spiking neurons," in *ESANN*, 2000, pp. 419–424.
- [29] P. O'Connor and M. Welling, "Deep spiking networks," *arXiv preprint arXiv:1602.08323*, 2016.
- [30] J. Wu, Y. Chua, M. Zhang, Q. Yang, G. Li, and H. Li, "Deep spiking neural network with spike count based learning rule," in *2019 International Joint Conference on Neural Networks (IJCNN)*. IEEE, 2019, pp. 1–6.
- [31] S. B. Shrestha and G. Orchard, "Slayer: Spike layer error reassignment in time," *arXiv preprint arXiv:1810.08646*, 2018.
- [32] W. Zhang and P. Li, "Spike-train level backpropagation for training deep recurrent spiking neural networks," *arXiv preprint arXiv:1908.06378*, 2019.
- [33] G. Bellec, D. Salaj, A. Subramoney, R. Legenstein, and W. Maass, "Long short-term memory and learning-to-learn in networks of spiking neurons," *arXiv preprint arXiv:1803.09574*, 2018.
- [34] W. Zhang and P. Li, "Temporal spike sequence learning via backpropagation for deep spiking neural networks," *arXiv preprint arXiv:2002.10085*, 2020.
- [35] X. Cheng, Y. Hao, J. Xu, and B. Xu, "Lisnn: Improving spiking neural networks with lateral interactions for robust object recognition," in *IJCAI*, pp. 1519–1525.
- [36] Z. Pan, J. Wu, M. Zhang, H. Li, and Y. Chua, "Neural population coding for effective temporal classification," in *2019 International Joint Conference on Neural Networks (IJCNN)*. IEEE, 2019, pp. 1–8.
- [37] J. C. Thiele, O. Bichler, and A. Dupret, "Spikegrad: An ann-equivalent computation model for implementing backpropagation with spikes," *arXiv preprint arXiv:1906.00851*, 2019.
- [38] J. Zhu, M. Jiang, M. Yang, H. Hou, and Y. Shu, "Membrane potential-dependent modulation of recurrent inhibition in rat neocortex," *PLoS Biol*, vol. 9, no. 3, p. e1001032, 2011.
- [39] A. Paszke, S. Gross, S. Chintala, G. Chanan, E. Yang, Z. DeVito, Z. Lin, A. Desmaison, L. Antiga, and A. Lerer, "Automatic differentiation in pytorch," 2017.
- [40] D. P. Kingma and J. Ba, "Adam: A method for stochastic optimization," *arXiv preprint arXiv:1412.6980*, 2014.
- [41] Y. LeCun, "The mnist database of handwritten digits," <http://yann.lecun.com/exdb/mnist/>, 1998.
- [42] G. Orchard, A. Jayawant, G. K. Cohen, and N. Thakor, "Converting static image datasets to spiking neuromorphic datasets using saccades," *Frontiers in neuroscience*, vol. 9, p. 437, 2015.
- [43] H. Xiao, K. Rasul, and R. Vollgraf, "Fashion-mnist: a novel image dataset for benchmarking machine learning algorithms," *arXiv preprint arXiv:1708.07747*, 2017.

- [44] A. Krizhevsky, "Learning multiple layers of features from tiny images," Tech. Rep., 2009.



Dongcheng Zhao received the B.Eng. degree in Information and Computational Science from Xi-Dian University, Xi'an, Shaanxi, China, in 2016. He is currently pursuing the PH.D. degree with the Institute of Automation, Chinese Academic of Sciences, Beijing, China. His current research interests include learning algorithms in spiking neural networks, thalamus-cortex interaction, visual object tracking, etc.



Yi Zeng obtained his Bachelor degree in 2004 and Ph.D degree in 2010 from Beijing University of Technology, China. He is currently a Professor and Deputy Director at Research Center for Brain-inspired Intelligence, Institute of Automation, Chinese Academy of Sciences (CASIA), China. He is also with the National Laboratory of Pattern Recognition, CASIA, and University of Chinese Academy of Sciences, China. He is a Principal Investigator at Center for Excellence of Brain Science and Intelligence Technology, Chinese Academy of Sciences, China. His research interests include cognitive brain computational modeling, brain-inspired neural networks, brain-inspired robotics, etc.



Yang Li received the B.Eng. degree in automation from Harbin Engineering University, Harbin, China, in 2019. He is currently pursuing the master's degree with the Institute of Automation, Chinese Academic of Sciences, Beijing, China. His current research interests include learning algorithms in spiking neural networks and cognitive computations.